Department of Physics

PHY-412: Physics of Galaxies

by
Peter Clegg
Revised by
Peter Williams and Bernard Carr

Chapter 5. Galaxian Demography

Table of Contents

CHAPTER 5: GALAXIAN DEMOGRAPHY

1. Introduction

So far, we have considered galaxies in isolation from each other. We should now look at the how galaxies are distributed in luminosity and real space. First, though, let us look at what samples of galaxies are available for study.

2. Samples of Galaxies

2.1 Photographic Atlases

There are two main photographic atlases of the sky – the Palomar Observatory Sky Survey (POSS) and the ESO-SERC Southern Sky Survey. The former covers the northern sky from the Schmidt telescope on Mount Palomar in California. It consists of 879 pairs of glass plates 6 by 6 degrees in extent. The blue band plates reach magnitude 21.1 and the red plates magnitude 20.0. The ESO-SERC Southern Sky Survey covers the southern sky from the Schmidt telescope at Siding Spring in New South Wales. Again, it is on 6 by 6 degree glass plates. More recently optical surveys such as the Sloan Digital Sky Survey (SDSS) have been carried out using modern CCD detectors.

2.2 Optical Catalogues

The two main galaxy – as opposed to general – catalogues are those of Shapley Ames, covering the northern sky down B~13, and Zwicky, also covering the northern sky but down to B~15. The New General Catalogue (NGC) and Upsala Galaxy Catalogue (UGC) also go down to this limit but include objects other than galaxies.

2.3 Infrared Surveys

The are several infrared surveys. The pioneering Caltech 2μm survey was carried out by Gerry Neugebauer and Eric Becklin in 1969 using a fairly primitive detector and a chart recorder. At the other end of the scale, the Infrared Astronomy Satellite (IRAS) mapped the entire sky at 12, 25, 60 and 120 μm in the mid-1980s and revealed several entirely new classes of object, including ultraluminous galaxies.

2.4 X-Ray Surveys

X-ray surveys have to be done from space because the Earth's atmosphere is opaque to these rays. The classic surveys of the 1970s, by the UHURU, Ariel V and HEAO-1 satellites, found mostly (a) active galaxies and quasars, and (b) diffuse hot gas in clusters of galaxies. The Einstein satellite, in the 1980s and the ROSAT mission in the 1990s found yet more AGN but were sensitive enough to see normal galaxies as well.

2.5 Radio Surveys

These are carried out with large telescopes on the ground. By using interferometry between telescopes separated by up to intercontinental distances, very high angular resolution can be achieved. The early (1960s) low-frequency surveys such as the third Cambridge (3C) and the Parkes (PKS) Australian surveys revealed mainly the classic doubles sources and quasars. The higher-frequency surveys of the 1970s revealed blazers while the very deep surveys of the 1980s and 1990s contain starburst galaxies.

2.6 Redshift Surveys

All the above surveys are two-dimensional; that is, they give merely the angular position of the source on the sky. If we are to get a three-dimensional picture, we need to measure the redshifts for a whole sample of galaxies. Major redshift surveys include:

- the Centre for Astrophysics (CfA) survey of all Zwicky galaxies in the north down to B ~ 14.5;
- the extended CfA survey, which has "slices" of sky down to B ~ 15.5;
- the Queen Mary, Durham, Oxford and Toronto (QDOT) all-sky survey of IRAS galaxies with $S(60\mu m) > 0.6$ Jy;
- the Stromlo-APM Redshift Survey,
- the Sloan Digital Sky Survey in N and S;
- the 2 Degree Field Galaxy Redshift survey (2dF GRS) in the South;

as well as several others over small areas of the sky.

3. Luminosities of Galaxies

3.1 Flux-Limited Surveys

3.1.1 Number Counts

Suppose for a moment that all galaxies have the same luminosity L. Such a galaxy at a distance r will be observed with a flux density S given by[1]

$$S = \frac{L}{4\pi r^2}. \qquad (3.1)$$

Alternatively, the distance $r(S)$ of a galaxy observed with flux density S is given by

$$r(S) = \left(\frac{L}{4\pi S}\right)^{1/2}. \qquad (3.2)$$

[1] In this Chapter we shall use S for the flux density instead of our previous notation F!

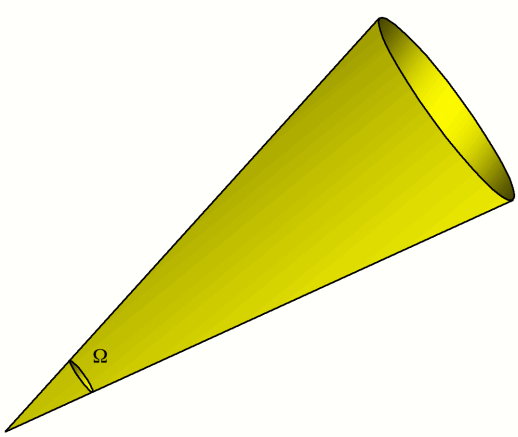

Figure 5-1. Observed volume of space.

Suppose that we observe a solid angle Ω on the sky, as shown in Figure 5-1. The volume $V(S)$ of space observed out to distance $r(S)$ is given by

$$V(S) \equiv \int_0^{r(S)} \left(r^2\Omega\right) dr = \frac{\Omega}{3} r^3(S) = \frac{\Omega}{3(4\pi)^{3/2}} L^{3/2} S^{-3/2} \tag{3.3}$$

Let the number of galaxies per unit volume of space be ϕ. Then the number $N(S)$ of galaxies observed to have flux density greater than S is given by

$$N(S) = V(S) \times \phi = \left[\phi \frac{\Omega}{3(4\pi)^{3/2}} L^{3/2}\right] S^{-3/2}. \tag{3.4}$$

That is, the observed number of galaxies brighter than a given flux density is inversely proportional to the three-halves power of that flux density[2].

You will object that galaxies do *not* all have the same luminosity. On the contrary, they have a wide range of values of L. Surprisingly perhaps, this does not alter the above conclusion! Let $\phi(L)dL$ be the number of galaxies per unit volume with luminosity in the range L to $L + dL$. $\phi(L)$ is called the *galaxy luminosity function*. Then, following the above argument, the number $dN(S,L)dL$ *of* galaxies whose luminosities lie in the range L to $L + dL$ and which are observed to have flux greater than S is given by

$$\begin{aligned} dN(S,L) &= V(S,L) \times \phi(L) \\ &\frac{\Omega}{3} r^3(S,L) \times \phi(L) \\ &= \phi(L) L^{3/2} \frac{\Omega}{3(4\pi)^{3/2}} S^{-3/2} \end{aligned} \tag{3.5}$$

where $r(S,L)$ is the distance at which a source of luminosity L will be observed with flux density S and $V(S,L)$ is the observed volume of space within $r(S,L)$. Integrating over all values of L, we get for $N(S)$, the *total* number observed brighter than S, regardless of their luminosity,

$$\begin{aligned} N(S) &= \int_L dN(S,L) \\ &= \left[\frac{\Omega}{3(4\pi)^{3/2}} \int_L \phi(L) L^{3/2} dL\right] \times S^{-3/2}. \end{aligned} \tag{3.6}$$

This shows that $N(S)$ is still inversely proportional to the three-halves power of S, regardless of the form of $\phi)L)$.

3.1.2 Redshift Surveys

How can we estimate $\phi(L)$? We have to allow for the fact that, whilst we can see very luminous galaxies a long way off, faint ones will only be seen if they are nearby. If we measure the distances r of individual galaxies[3], we can determine their luminosities directly from their measured flux densities: according to equation (3.1),

$$L = 4\pi r^2 S.$$

Suppose we survey a solid angle Ω of the sky down to some limiting flux density $S_{\rm lim}$. That is, we count all galaxies within this solid angle whose flux density exceeds $S_{\rm lim}$. In such a survey, the distance $r_{\rm max}$ out to which a galaxy of luminosity L could still be seen is given, according to equation (3.2), by

$$r_{\rm max}(L) = \left(\frac{L}{4\pi S_{\rm min}}\right)^{1/2}. \tag{3.7}$$

A galaxy of luminosity L will therefore appear in the survey provided that it is in the volume $V_{\rm max}(L)$ of space given by

$$V_{\rm max}(L) = \frac{r_{\rm max}^3(L)}{3}\Omega. \tag{3.8}$$

The total number $N(L)dL$ of galaxies appearing in the survey, with luminosities in the range L to $L + dL$, is therefore given by

$$N(L)dL = V_{\rm max}(L) \times \phi(L) dL. \tag{3.9}$$

Re-arranging equation (3.9), we get

[2] Our derivation assumes (a) that space is Euclidean and static and (b) that $\phi(S)$ is independent of time. We shall see later that we shall have to modify these assumptions for objects at great distances.

[3] For all but the nearest galaxies, we do this by measuring the galaxy's redshift and using Hubble's law. Because each galaxy has its own peculiar velocity superimposed upon the Hubble velocity. this leads to some error in r. Alternatively. if we are trying to determine $\phi(L)$ for a cluster of galaxies, we can assume that they are all at the same distance.

$$\phi(L)dL = \frac{N(L)}{V_{\max}(L)}dL = 3(4\pi)^{3/2}\frac{N(L)}{\Omega}\left(\frac{L}{S_{\lim}}\right)^{-3/2}dL \qquad (3.10)$$

In the last line we used equations (3.7) and (3.8) to show what is required to determine $\phi(L)$. The observational procedure for determining $\phi(L)$ is, therefore:

(a) observe a solid angle Ω on the sky and catalogue all galaxies within it above the limiting flux density $S_{\lim}$;

(b) determine the redshift and hence the distance of each galaxy within the sample;

(c) calculate the luminosity of each galaxy and the corresponding maximum volume $V_{\max}(L)$ using equations (3.7) and (3.8);

(d) divide the sample into bins of width ΔL in luminosity;

(e) for each bin, calculate $\phi(L)\Delta L$ from

$$\phi(L)\Delta L = \frac{N(L)\Delta L}{V_{\max}(L)}; \qquad (3.11)$$

(f) draw a smooth curve from the resulting histogram of $\phi(L)\Delta L$ to give an estimate of $\phi(L)$.

3.2 The Luminosity Function

3.2.1 The Optical Luminosity Function

3.2.1.1 The Schechter Function

The result of carrying out the procedure of section 3.1.2 is that we find $\phi(L)$ to be well represented by the *Schechter function*:

$$\phi(L)dL = \frac{\phi_*}{L_*}\left(\frac{L}{L_*}\right)^{-\alpha} e^{-(L/L_*)}dL\,, \qquad (3.12)$$

where ϕ_*, L_* and α are constants. The observed values of these constants depend upon the type of galaxy and its environment but overall values are:[4]

$$\alpha \sim 1.1;$$
$$\phi_* \sim 0.015\ \mathrm{Mpc}^{-3}; \qquad (3.13)$$
$$L_* \sim 10^{10} h^{-2}\ \mathrm{L_{sun}}.$$

The Schechter function is plotted in Figure 5-2.

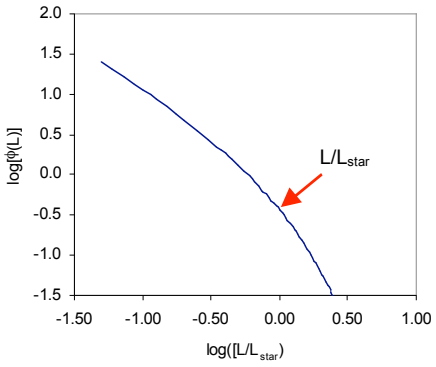

Figure 5-2. The Schechter luminosity function.

In the same way that we introduced $\nu S(\nu)$ – the SED – as a crude measure of the power emitted by a galaxy at frequency ν, it is convenient to employ the *luminosity distribution* $L\phi(L)$ as a measure of the number of galaxies with luminosity L. We have, from equation (3.12),

$$L\phi(L) = \phi_*\left(\frac{L}{L_*}\right)^{1-\alpha} e^{-(L/L_*)}, \qquad (3.14)$$

which is plotted in Figure 5-3. If we like, we can regard L_* as the luminosity of a "typical" galaxy and ϕ_* as the number of galaxies per unit volume with luminosity close to L_*. In this sense, a typical galaxy has a luminosity of about 10^{10} $\mathrm{L_{sun}}$, like our own, and there is about one of them in every hundred cubic megaparsecs of space. We should realise, however, that there is an ever-increasing number of faint galaxies – dwarfs – and that there are rather few galaxies with luminosity greater than L_*.

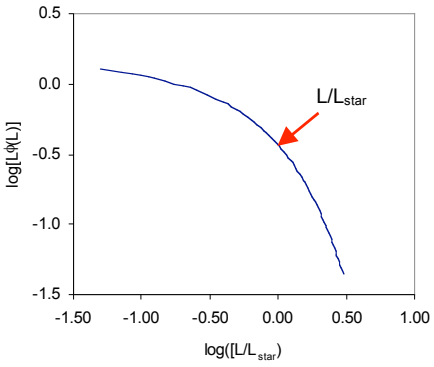

Figure 5-3. The Schechter luminosity distribution.

Given that the observed luminosity function has the Schechter form, we can now see what the distribution of luminosities in the flux-limited survey looks like. From equations (3.7), (3.8) and (3.9), we have

[4] Recall that the current value for h is now well determined as 0.7.

$$N(L) = V_{\max}(L) \times \phi(L)$$
$$= \frac{\Omega}{3}\left(\frac{L}{4\pi S_{\min}}\right)^{3/2} \frac{\phi_*}{L_*}\left(\frac{L}{L_*}\right)^{-\alpha} e^{-(L/L_*)} \qquad (3.15)$$
$$= \frac{\Omega}{3}\phi_* L_*^{1/2}(4\pi S_{\min})^{-3/2}\left(\frac{L}{L_*}\right)^{3/2-\alpha} e^{-(L/L_*)}.$$

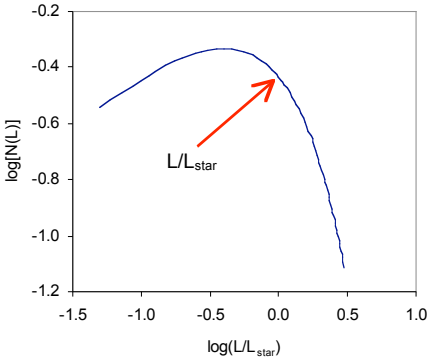

Figure 5-4. Numbers in flux-limited survey.

$N(L)$ is plotted in Figure 5-4. The number of galaxies in the survey can be seen as a function of luminosity near[5] L_*. Thus, the survey – our *picture* of the universe – is dominated by luminous galaxies, even though space itself is dominated by dwarfs[6].

3.2.1.2 The Total Number Density of Galaxies

In principle, we should be able to obtain the total number of galaxies per unit volume N_{galaxies} by integrating the observed luminosity function over all luminosities:

$$N_{\text{galaxies}} = \int \phi(L)\,dL\,. \qquad (3.16)$$

Unfortunately, if we substitute the Schechter function for $\phi(L)$, the integral diverges at the low-luminosity end[7]. At face value, this implies that space is infinitely full of infinitesimally dull galaxies. In reality, we infer that the luminosity function must steepen somewhere towards the low end. Best estimates are that

$$N_{\text{galaxies}} \sim 10^{-2} h^3 \text{ Mpc}^{-3}\,. \qquad (3.17)$$

Relation (3.17) means that, on average, each galaxy occupies a volume V_{galaxy} given by

$$V_{\text{galaxy}} = \frac{1}{N_{\text{galaxy}}} \sim 100 h^{-3}\text{Mpc}^3\,, \qquad (3.18)$$

so that galaxies are typically separated by a distance r_{galaxies} given by

$$r_{\text{galaxies}} \sim V_{\text{galaxies}}^{1/3} \sim 5h^{-1}\text{Mpc}\,. \qquad (3.19)$$

3.2.1.3 The Total Luminosity Density of Galaxies

The total luminosity density L_{total} is given by

$$L_{\text{total}} = \int L\phi(L)\,dL\,. \qquad (3.20)$$

For the Schechter function, this converges at both ends and we find that

$$L_{\text{B,total}} \sim 2\times 10^8 h \text{ L}_{\text{sun}}\text{Mpc}^{-3}\,. \qquad (3.21)$$

If we assume a mass-luminosity ratio for galaxies, we can estimate the mass-density ρ_{galaxies} of matter in galaxies:

$$\rho_{\text{galaxies}} = L_{\text{total}} \times \left\langle \frac{M}{L} \right\rangle_{\text{galaxies}}\,. \qquad (3.22)$$

As we saw in chapter 2, the mass-luminosity ratio of galaxies is not well defined. If we use the value for spiral galaxies, derived from rotation curves, we get from equations (3.9) and (3.22),

$$\rho_{\text{galaxies}} \sim 2\times 10^8 h \times 10h \text{ M}_{\text{sun}}\text{Mpc}^{-3}$$
$$\sim 2\times 10^9 h^2 \text{ M}_{\text{sun}}\text{Mpc}^{-3} \qquad (3.23)$$
$$\sim 1.5\times 10^{-28} h^2 \text{ kg m}^{-3}.$$

If we use the value for ellipticals, on the other hand, we get

$$\rho_{\text{galaxies}} \sim 2\times 10^8 h \times 40h \text{ M}_{\text{sun}}\text{Mpc}^{-3}$$
$$\sim 8\times 10^9 h^2 \text{ M}_{\text{sun}}\text{Mpc}^{-3} \qquad (3.24)$$
$$\sim 6\times 10^{-28} h^2 \text{ kg m}^{-3}.$$

We may tentatively conclude that the total mass-density of the universe in the form of *galaxies*[8] lies somewhere in this range. These figures should be compared with the critical density

$$\rho_{\text{crit}} = 1.8\times 10^{-26} h^2 \text{ kg m}^{-3}\,, \qquad (3.25)$$

which must be exceeded to close the universe.

3.2.2 The Luminosity Function at other Wavelengths

At radio and X-ray wavelengths, surveys are dominated by active galaxies. The form of the luminosity function is

[5] In fact at about 0.4 L_*.

[6] This is the same effect as we see when we look at the night sky. Although low-mass, low luminosity stars dominate the stellar population of the galaxy, our flux-limited eyes see mainly luminous stars.

[7] This is because α in the Schechter function is greater than unity. If it were less than unity, the integral would diverge at the high end.

[8] We shall see shortly that there is a significant amount of matter in between galaxies.

$$\phi(L) \propto L^{-3}. \qquad (3.26)$$

This power-law is steeper than that for the optical band but there is no exponential cut-off. At the far-infrared wavelengths surveyed by the IRAS satellite, the function has the form

$$\phi(L) \propto L^{-\alpha},\ \alpha \sim 1-3, \qquad (3.27)$$

with the power falloff getting steeper as the luminosity increases. At low luminosities therefore, the function is flat as in the optical. At high luminosities, it is steep like active galaxies.

4. Groups and Clusters of Galaxies

4.1 A Tour of Clustering (cf. ref. [1])

4.1.1 The Galaxy and its Satellites

Let us work up from the smallest associations to the biggest. Our own Galaxy, some 30 kpc in diameter, is accompanied by several satellites, the two largest being the Large Magellanic Cloud (LMC) at a distance of about 55 kpc and the Small Magellanic Cloud (SMC) about 67 kpc away, both irregular galaxies. Other dwarf satellites are Sculptor, Draco and Ursa Minor, all between 50 and 100 kpc away.

4.1.2 The Local Group

Excluding the Magellanic Clouds, there are three major players in the local group, listed in Table 5.1, which also gives their types, magnitudes, distances and velocities[9] with respect to the Galaxy. Note that both M31 (Andromeda) and M33 are approaching us, showing that they are too close for their velocities to be dominated by the Hubble flow.

Table 5.1. The Local Group

Galaxy	Type	M_V	Distance (kpc)	Velocity (km s^{-1})
Galaxy	Sbc	-20.5	-	-
M31	Sbc	-21.2	710	-299
M33	Sc	-19.1	850	-183

The local group also contains about 26 dwarf galaxies[10] – mostly irregular and elliptical – with apparent magnitudes down to about –7.9. Their distances range out to about 600 kpc.

4.1.3 Nearby Groups

Table 5.2. Nearby Groups

Group	Distance (Mpc)	Velocity (km s^{-1})
Sculptor	1.9	-59
M81	2.9	298
NGC5128	4.3	695
Canes Venatici I	5.1	574
M101	6.8	498

Table 5.2 lists the major nearby groups, which are similar to the Local Group, with a few large galaxies and lots of small ones. The quoted distances and velocities are the mean values for the group. Note that the velocities are still governed by local dynamics rather than the Hubble flow. NGC5128, for example, has 2.5 times the velocity predicted for $h = 0.65$. There are about ten other small groups out to about 15 Mpc.

4.1.4 The Virgo Cluster

The Virgo Cluster, which dominates the northern sky and of which we are a part, contains thousands of galaxies. The centre of the cluster is 13-20 Mpc away and velocities are in the range 1200±500 km s^{-1}, now Hubble dominated.

4.1.5 Other Nearby Clusters[11]

There are several clusters as striking as Virgo out to a redshift of 0.03, corresponding to a velocity of recession of 10,000 km s^{-1} and a distance of 100h Mpc. These clusters are listed in Table 5.3.

Table 5.3. Local Clusters

Cluster	Velocity (km s^{-1})	Distance (h^{-1} Mpc)
Centaurus	3,500	350
Hydra	3,500	350
Pisces	5,000	500
Perseus	5,200	520
Coma	7,000	700
Hercules	10,000	1,000

4.1.6 Superclusters

Superclusters are rather loosely defined as clusters of clusters on scales of 20 – 100 Mpc, with very large voids in between. Examples are:

Local Supercluster
Perseus-Pisces-A569
Coma-A1367
Hydra-Centaurus
Hercules-A2197-A2199

[9] Velocities are conventionally given a positive sign if they are receding from us.

[10] Remember that most galaxies are dwarfs.

[11] Not that the radius of the observable universe is about 3000/h Mpc.

It is not clear, however, that the concept of superclusters is useful or has any meaning (see later).

4.2 Rich Clusters of Galaxies

4.2.1 Abell Clusters

George Abell, one of the team carrying out the POSS in the 1940s, defined the concept of a rich cluster as one in which there was no doubt that the galaxies clustered on the plate were really part of a physical entity. He compiled a statistically complete[12] catalogue of 1682 clusters (necessarily in the northern hemisphere) and assigned them to classes according to their "richness", defined by a rather complicated criterion. Let the *third* brightest member of the cluster have magnitude m_3. Then the richness of the cluster is determined by the number of its members, within 1.7/z arcminutes – equivalent to 1.5 h^{-1} Mpc – of the cluster centre, brighter then $m_3 + 2$. In terms of flux density, if the third brightest member has flux density S_3, then the richness is determined by the number of galaxies in the cluster with flux-densities greater than $6.3 \times S_3$. The complete classification is given in Table 5.4. Note that, in order to count as Abell-rich[13], a cluster must have at least 50 galaxies brighter than $m_3 + 2$.

The Abell scheme has now been extended to the southern sky using the ESO-SERC Southern Sky Survey and the combined catalogue contains 4073 clusters.

Table 5.4. Abell Richness Classes

Richness Class	Number of Galaxies brighter than $m_3 + 2$	Number of Clusters
1	50 – 79	1224
2	80 – 129	383
3	130 – 199	68
4	200 – 299	6
5	>300	1

It is found that the number density $N_{\rm Abell}$ of Abell clusters is given by

$$N_{\rm Abell} = 10^{-5} h^3 \ {\rm Mpc}^{-3}, \qquad (4.1)$$

so that, according the argument of section 3.2.1.2, the average separation $r_{\rm Abell}$ of cluster centres is given by

$$r_{\rm Abell} \sim N_{\rm Abell}^{-1/3} \sim 50 h^{-1} {\rm Mpc}, \qquad (4.2)$$

ten times the average separation of galaxies themselves.

4.2.2 Properties of Rich Clusters

4.2.2.1 Contents of the Clusters

Abell divided his clusters into regular and irregular types. Regular clusters:

- are circularly (and therefore probably spherically) symmetric;
- are concentrated towards the centre;
- contain very few spirals and consist primarily of elliptical and S0 galaxies.

They are the easier to study. Examples are Coma and Corona Borealis. Irregular clusters, such as Hercules and Virgo, are not centrally concentrated and contain more spirals. Oemler [2] distinguished the Abell types given in Table 5.5, which gives a brief description of the types and the relative proportions of elliptical, lenticular and spiral galaxies in each type.

Table 5.5.

Type	Content	E:S0:S
cD	Dominant cD galaxy (sometimes two)	3:4:2
Spiral-rich	Similar to field galaxies	1:2:3
Spiral-poor	No dominant cD galaxy	1:2:1

A cD galaxy is a giant elliptical with an extended stellar envelope up to 100 kpc in size. They are found only in regions of significantly enhanced galaxian density, suggesting that they come about form the merger of lesser galaxies.

4.2.2.2 The Density Profile of Rich Clusters

If we measure the surface number density $s(\theta)$ of galaxies – that is, the number of galaxies per unit solid angle – in a rich cluster, as a function of angular distance θ from the centre of the cluster, we find that it can be well fitted by

$$s(\theta) = \frac{s_{\rm o}}{1 + (\theta/\theta_{\rm core})^2}, \qquad (4.3)$$

where $s_{\rm o}$ is the surface number density at the centre of the cluster and $\theta_{\rm core}$ is the angular radius at which the density fall to half its central value. If we assume that the cluster is spherically symmetric, then the *spatial* number density $n(r)$ corresponding to (4.3) is given by

$$n(r) = \frac{n_{\rm o}}{\left[1 + \left(2^{2/3} - 1\right)\ (r/r_{\rm core})^2\right]^{3/2}}, \qquad (4.4)$$

where $n_{\rm o}$ is the number density at the centre of the cluster and $r_{\rm core}$ is the core radius at which the density falls to half its central value. Typical values obtained from observations of rich clusters are:

$$\begin{aligned} n_{\rm o} &\sim 3000 \ {\rm Mpc}^{-3}; \\ r_{\rm core} &\sim 0.15 - 0.4 \ {\rm Mpc}. \end{aligned} \qquad (4.5)$$

For the Coma cluster, $r_{\rm core}$ is 220 kpc.

[12] In fact, the complete catalogue also restricts the redshift range to between 0.02 and about 0.2.

[13] A class 0 is sometimes introduced for clusters with 30 to 49 galaxies brighter than $m_3 + 2$, but Abell's catalogue is not complete for these.

4.2.2.3 Binding of Clusters

By measuring the redshifts of individual galaxies, we can determine the root-mean-squared line-of-sight velocity $\left\langle v_r^2 \right\rangle$ of the galaxies with respect to the centre of the cluster. A typical value is 1000 km s^{-1}. Assuming that the velocity distribution is isotropic, we have for the total mean-squared velocity

$$\left\langle v^2 \right\rangle = 3\left\langle v_r^2 \right\rangle \quad \text{i.e.} \quad \left\langle v^2 \right\rangle^{1/2} = \sqrt{3}\left\langle v_r^2 \right\rangle^{1/2}. \tag{4.6}$$

A typical velocity $\langle v \rangle$ of a galaxy in a cluster is, therefore, some 1,700 km s^{-1}. The time τ_{crossing} for a galaxy to cross the cluster is given by

$$\tau_{\text{crossing}} \sim \frac{r_{\text{cluster}}}{\langle v \rangle}. \tag{4.7}$$

Taking the size of the cluster to be ten times its core radius, say, we have

$$\tau_{\text{crossing}} \sim 10\frac{r_{\text{core}}}{\langle v \rangle}. \tag{4.8}$$

or, putting in numbers,

$$\tau_{\text{crossing}}(\text{y}) \sim 10^{10}\frac{r_{\text{core}}(\text{Mpc})}{\langle v \rangle\left(10^3 \text{ km s}^{-1}\right)}. \tag{4.9}$$

Typically, τ_{crossing} is about 10^9 years and the galaxies have had time to make many crossings in the life of the universe. This is evidence that the galaxies we see in the cluster are bound since otherwise the cluster would have dispersed by now.

4.2.2.4 Cluster Relaxation Times

In chapter 3, we derived an expression for the time $\tau_{\text{collision}}$ between collisions of objects of moving randomly. In a notation suitable for our present case, we have

$$\tau_{\text{collision}} = \frac{1}{4\pi R_{galaxy}^2 n\langle v \rangle}, \tag{4.10}$$

where R_{galaxy} is the radius of an individual galaxy and n is the number-density of galaxies in the cluster. Putting in numbers, we get

$$\tau_{\text{collision}}(y) = \frac{7.6\times10^{16}}{R_{galaxy}^2(\text{kpc})n(\text{Mpc}^{-3})\langle v \rangle(km\,s^{-1})} \tag{4.11}$$

Taking $R_{\text{galaxy}} \sim 15$ kpc, $\left\langle v^2 \right\rangle^{1/2} \sim 2000$ km s^{-1} and $n \sim 3000$ Mpc^{-3} for the cores of clusters, we find that $\tau_{\text{collision}}$ is a few times 10^7 years, so that many collisions have taken place in the lifetime of the cluster. Even in the outer regions, where the density has fallen by an order of magnitude, collisions will still be frequent on a cosmological time scale. We may therefore consider these rich clusters to be dynamically relaxed. (i.e. there has been plenty of time for the galaxies within the cluster to interact gravitationally with each other and share their energies.)

4.2.2.5 The Isothermal Sphere

Equation (4.4) is a good approximation to what we should expect to find if cluster were an *isothermal sphere*. What do we mean by this? Consider a perfect gas at temperature T. The mean kinetic energy K of the molecules making up the gas is given by

$$K \equiv \frac{1}{2}\mu m_{\text{H}}\left\langle v_{\text{molecules}}^2 \right\rangle = \frac{3}{2}kT, \tag{4.12}$$

where μ is the mean molecular weight of the molecules, m_{H} is the mass of the hydrogen atom and $\langle v^2_{\text{molecules}} \rangle$ is the mean-squared velocity of the molecules.

If the cluster is dynamically relaxed, that is, there has been plenty of time for the galaxies within the cluster to interact gravitationally with each other and share their energies, as discussed above, then we should expect that their average kinetic energy is the same everywhere in the cluster. By analogy with the gas of molecules, therefore, we should expect to be able to model the cluster as a perfect gas of galaxies with an effective temperature T_{cluster} given by

$$\frac{1}{2}m_{\text{galaxies}}\left\langle v^2 \right\rangle = \frac{3}{2}kT_{\text{cluster}}, \tag{4.13}$$

where m_{galaxies} is the average mass of a galaxy in the cluster and $\langle v^2 \rangle$ is their mean-squared velocity.

If this "thermal" energy is supporting it against gravitational collapse, then the cluster – assumed spherically symmetric – must obey the *equation of hydrostatic equilibrium*[14]:

$$\frac{dp(r)}{dr} = -\frac{GM(r)\rho(r)}{r^2} \tag{4.14}$$

where $p(r)$ and $\rho(r)$ are respectively the density and effective pressure exerted by the galaxies at radius r from the centre of the cluster and $M(r)$ is the mass of the cluster interior to r.

Treating the galaxies as a perfect gas enables us to find the pressure,

$$p = nkT = \frac{\rho}{m}kT, \tag{4.15}$$

so we can rewrite equation (4.14) as

$$\frac{d}{dr}\left[\frac{\rho(r)}{m_{\text{galaxies}}}kT_{\text{cluster}}\right] = -\frac{GM(r)\rho(r)}{r^2} \tag{4.16}$$

[14] See, for example, the course PHY-212 *Physics and Astronomy of Stars*.

or, since for this *isothermal* gas $T_{\rm cluster}$ is the same everywhere and therefore independent of r ,

$$\frac{r^2}{\rho(r)}\frac{d}{dr}[\rho(r)] = -\frac{Gm_{\rm galaxies}}{kT_{\rm cluster}}M(r). \qquad (4.17)$$

This is a differential equation in the unknown density $\rho(r)$, but also involves the unknown mass $M(r)$ which can only be found once the density is known by integrating out to r.[15] However the derivative of $M(r)$ is a simple function of r and $\rho(r)$, which suggests we differentiate both sides of equation (4.17), to get a differential equation in $\rho(r)$ alone:

$$\begin{aligned}\frac{d}{dr}\left\{\frac{r^2}{\rho(r)}\frac{d}{dr}[\rho(r)]\right\} &= -\frac{Gm_{\rm galaxies}}{kT_{\rm cluster}}\frac{dM(r)}{dr}\\ &= -\frac{Gm_{\rm galaxies}}{kT_{\rm cluster}}\times 4\pi r^2\rho(r)\cdot\\ &= -12\pi G\frac{r^2\rho(r)}{\langle v^2\rangle},\end{aligned} \qquad (4.18)$$

where we have used equation (4.13) to eliminate *both* the unknowns $T_{\rm cluster}$ and m_g in favour of the measured quantity $\langle v^2\rangle$.

We can now recast this equation into dimensionless form by writing the density in units of the central density ρ_0 and the radial coordinate in units of some convenient radius α. Distributing these factors equally on both sides of equation (4.18) gives

$$\begin{aligned}&\frac{d}{d(r/\alpha)}\left[(r/\alpha)^2\frac{1}{(\rho/\rho_0)}\frac{d(\rho/\rho_0)}{d(r/\alpha)}\right]\\ &= -\left(\frac{12\pi G}{\langle v^2\rangle}\alpha^2\rho_0\right)(r/\alpha)^2(\rho/\rho_0),\end{aligned} \qquad (4.19)$$

which is now in dimensionless form. Since we are free to choose the radius α at our convenience the obvious choice is to make the bracketed constant on the right side of equation (4.19) unity. The equation is then

$$\frac{d}{d\xi}\left[\xi^2\frac{1}{\omega}\frac{d\omega}{d\xi}\right] = -\xi^2\omega\,, \qquad (4.20)$$

where

$$\xi := \frac{r}{\alpha};\quad \omega := \frac{\rho(r)}{\rho_o};\quad \alpha^2 = \frac{\langle v^2\rangle}{12\pi G\rho_o}\,. \qquad (4.21)$$

Notice that since the mass density $\rho(r)$ is related to the number density $n(r)$ by

$$\rho(r) = n(r)\times m_g\ ,\ \textit{i.e.}\ \ \omega = \frac{\rho}{\rho_0} = \frac{n\,m_g}{n_0\,m_g} = \frac{n}{n_0}, \qquad (4.22)$$

so that (4.20) is equally an equation for $n(r)/n_o$, where n_o is the central-number density.

Equation (4.20) is a non-linear differential equation and must be solved numerically; its solution $\omega(r)$ is plotted against $\xi(r)$ in Figure 5-5 as a full line.

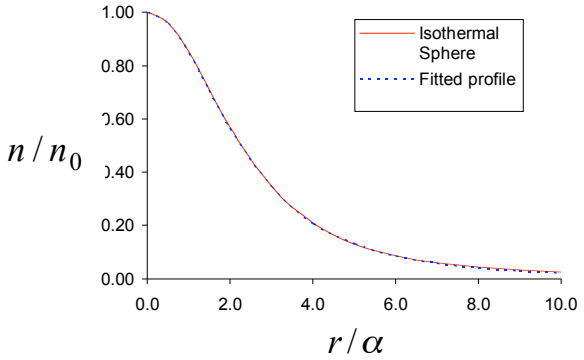

Figure 5-5. Cluster number density profiles

We can now evaluate α from this graph by remembering that the *isothermal core radius* $r_{\rm core}$ is the radius at which the number density is half the central density - see equation (4.4). From Figure 5-5 this happens at $r/\alpha = 2.25$; hence $\alpha = r_{\rm core}/2.25$, where $r_{\rm core}$ is already known from fitting density profile *observations* with equations (4.3) and (4.4). With α now known we can also plot in Figure 5-5 the profile (4.4) which fits the observed number density – the dashed curve. It can be seen that there is very good agreement with the isothermal sphere profile. We may therefore conclude that rich clusters are remarkably well described as isothermal spheres.

Having now determined α we can use the *measured* mean-squared line-of-sight velocity $\langle v_r^2\rangle$ of the galaxies in the cluster in the third of equations (4.21) to obtain the central density ρ_0,[16]

$$\begin{aligned}\rho_o &= \frac{3\langle v_r^2\rangle}{12\pi G\alpha^2} = \frac{\langle v_r^2\rangle}{4\pi G(r_{\rm core}/2.25)^2}\\ &= 1.2\frac{\langle v_r^2\rangle}{Gr_{\rm core}^2}.\end{aligned}\ . \qquad (4.23)$$

The central density can therefore be obtained directly from observation.

The total mass of the cluster can now be obtained by integrating the profile for an isothermal sphere out to

[15] $M(r) = \int_0^r \rho(r')4\pi r'^2 dr'$ gives $\dfrac{dM(r)}{dr} = \rho(r)4\pi r^2$

[16] Since we can only measure the line-of-sight velocity squared dispersion $\langle v_r^2\rangle$ we assume an isotropic velocity distribution to write $\langle v^2\rangle = 3\langle v_r^2\rangle$ to estimate the full 3-dimensional value.

some maximum radius, say $\sim 10 r_{\rm core}$.[17] For the Coma cluster, this gives a mass of $1.8 \times 10^{15}\, h^{-1}\, M_{\rm sun}$. Alternatively, the mass can be estimated by applying the virial theorem to the cluster (cf. chapter 3). Typically, these dynamical methods give masses of the order of $10^{15}\, M_{\rm sun}$ for rich clusters.

4.2.2.6 Intracluster Gas

As we saw at the beginning of this chapter, X-ray surveys revealed diffuse emission from clusters. The gas responsible for this emission is at temperatures of 10^7 – 10^8 K. Let us suppose that this gas is in hydrostatic equilibrium in the gravitational potential of the cluster so that its pressure $p(r)$ and density $\rho(r)$ at distance r from the centre of the cluster – assumed spherically symmetric – are related by the equation of hydrostatic equilibrium (4.14). We can use this equation to get a rough estimate of the pressure of the gas $p_{\rm centre}$ at the centre of the cluster. We approximate the left-hand side of the equation by

$$\frac{dp}{dr} \sim \frac{p_{\rm outside} - p_{\rm centre}}{r_{\rm cluster}} \approx -\frac{p_{\rm centre}}{r_{\rm cluster}}, \qquad (4.24)$$

where the pressure $p_{\rm outside}$ outside the cluster is taken to be negligible compared with that at the centre. The right hand side of equation (4.14) can be approximated as

$$-\frac{GM(r)}{r^2}\rho(r) \sim -\frac{GM_{\rm cluster}}{r_{\rm cluster}^2}\rho_{\rm centre}. \qquad (4.25)$$

From relations (4.24) and (4.25), we get

$$\frac{p_{\rm centre}}{r_{\rm cluster}} \sim \frac{GM_{\rm cluster}}{r_{\rm cluster}^2}\rho_{\rm centre}, \qquad (4.26)$$

or

$$p_{\rm centre} \sim \frac{GM_{\rm cluster}}{r_{\rm cluster}}\rho_{\rm centre}. \qquad (4.27)$$

If the gas is in thermal equilibrium[18] at temperature T, then we can use equation (4.15) to obtain

$$p = \frac{\rho}{\mu m_{\rm H}} kT, \qquad (4.28)$$

where μ is the mean molecular weight of the gas and $m_{\rm H}$ is the mass of the hydrogen atom. Substituting from (4.28) into (4.27), we get for the central temperature $T_{\rm centre}$,

$$kT_{\rm centre} \sim \frac{GM_{\rm cluster}\mu m_{\rm H}}{r_{\rm cluster}} \qquad (4.29)$$

which we can use to estimate the mass of the cluster. Putting in numbers, we get

$$M_{\rm cluster}(\mathrm{M_{sun}}) \sim 3.7\times 10^{14}\, r_{\rm cluster}(\mathrm{Mpc})\, T_{\rm centre}\left(10^8\,\mathrm{K}\right) \qquad (4.30)$$

where I have taken μ to be about 0.5, appropriate for ionised primordial gas. For a typical cluster size of a few Mpc, this gives masses of the order of $10^{15}\, M_{\rm sun}$, in good agreement with previous estimates.

In fact, we can do much better than this. The equation of hydrostatic equilibrium (4.14) can be combined with the perfect gas equation (4.28) to give

$$M(r) = -\frac{kT(r)}{G\mu m_{\rm H}} r^2 \left[\frac{1}{\rho(r)}\frac{d\rho}{dr} + \frac{1}{T(r)}\frac{dT}{dr}\right]. \qquad (4.31)$$

Detailed X-ray observations can determine the density and temperature of the gas, as a function of the distance from the centre of the cluster, and thus provide a detailed profile of the mass distribution. Again the results are in good agreement with other methods.

The total mass of the cluster is typically several times the mass in its constituent galaxies.

4.3 Statistics of Clustering

4.3.1 The Probability Functions

Let $P(\mathbf{r})dV$ be the probability that we find a galaxy within volume dV at point $\mathbf{r}$ in space, where $\mathbf{r}$ is measured from an arbitrary origin, as shown in Figure 5-6. If the distribution of galaxies is random, and if there are ϕ galaxies per unit volume, then

$$P(\mathbf{r}) = \phi. \qquad (4.32)$$

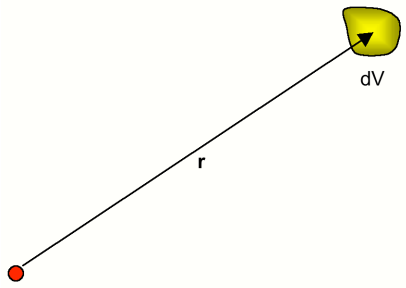

Figure 5-6. Probability of finding single galaxy.

[17] This is physically reasonable as the cluster does not extend out to infinity. This integral would diverge if it was continued out to infinity so this cut-off has to be applied (cf. Longair, *loc. cit.*)

[18] In fact, the X-ray observations show considerable variation in temperature. In particular, the gas in towards the centre of the cluster is significantly cooler that that outside. Nevertheless, the approximation is adequate for our rough estimate of the cluster mass.

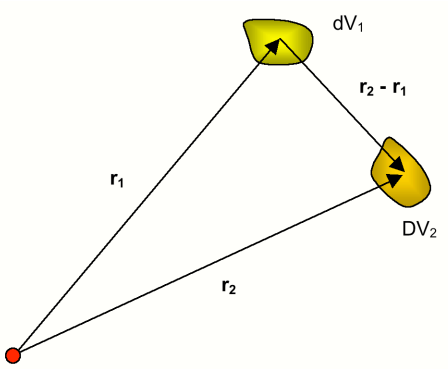

Figure 5-7. Probability of finding pair of galaxies.

Now consider the probability $P(\mathbf{r}_1,\mathbf{r}_2)dV_1dV_2$ of finding a galaxy within volume dV_1 at $\mathbf{r}_1$ *and* another galaxy within dV_2 at $\mathbf{r}_2$, as shown in Figure 5-7. By Bayes' law, we have

$$P(\mathbf{r}_1,\mathbf{r}_2) = P(\mathbf{r}_2|\,\mathbf{r}_1)\,P(\mathbf{r}_1) \tag{4.33}$$

where $P(\mathbf{r}_2|\,\mathbf{r}_1)dV_1dV_2$ is the *conditional probability* of finding a galaxy within dV_2 at $\mathbf{r}_2$, *given* that there is already one within dV_1 at $\mathbf{r}_1$. If the distribution of galaxies were entirely random, then the probability of finding a galaxy within dV_2 at $\mathbf{r}_2$ will be completely independent of the presence of the galaxy within dV_1 at $\mathbf{r}_1$. In that case

$$P(\mathbf{r}_2|\,\mathbf{r}_1) = P(\mathbf{r}_2) = \phi\,, \tag{4.34}$$

and

$$P(\mathbf{r}_1,\mathbf{r}_2)dV_1dV_2 = \phi^2 dV_1dV_2\,, \tag{4.35}$$

Suppose that this is not the case but that the probability of finding the second galaxy *is* dependent on the presence of the first. If space is isotropic, then $P(\mathbf{r}_2|\,\mathbf{r}_1)$ will depend only on the *magnitude* r of the difference between $\mathbf{r}_1$ and $\mathbf{r}_2$:

$$P(\mathbf{r}_2|\,\mathbf{r}_1) = P(|\mathbf{r}_2 - \mathbf{r}_1|) = P(r). \tag{4.36}$$

4.3.2 The Two-Point Correlation Function

Let us write $P(r)$ in the form

$$P(r) = \phi[1 + \xi(r)]. \tag{4.37}$$

$\xi(r)$ is called the *two-point correlation function* because it is a measure of the probability of finding galaxies at two different points in space. Note that, if $\xi(r)$ is zero, then $P(r)$ is independent of r and is equal to ϕ. This means that the probability of finding the second galaxy is independent of the presence of the first. $\xi(r)$ therefore measures the *excess* probability, above random, of finding a second galaxy near the first. Note that if $\xi(r) > 0$, then the probability is greater than random, indicating that galaxies tend to cluster together. If, on the other hand, $\xi(r) < 0$, galaxies tend to avoid each other and we have anti-clustering.

A statistical analysis of galaxy-pairs gives

$$\xi(r) = \left(\frac{r}{r_o}\right)^{-\gamma}, \quad \begin{matrix}\gamma = 1.77 \pm 0.10 \\ r_o = 5\ \text{Mpc}\end{matrix}, \tag{4.38}$$

so that $\xi(r)$ is positive as we should expect. The result (4.38) shows that the probability of finding another galaxy at 1 Mpc from another is 12 times the random probability and, even at 10 Mpc, is 1.2 times greater than if the distribution were random.

We find that $\xi(r)$ given by (4.38) is the same everywhere except in rich clusters: it is a *universal* clustering function. Note that it is *scale-free*. It has no characteristic scale length that would determine a typical size for clusters; it merely goes on decreasing indefinitely. This is what we should expect if it is determined by gravity, which itself has no characteristic scale length.

We do not observe the three-dimensional function $\xi(r)$ directly, of course. We use two-dimensional atlases or catalogues to estimate the probability $P(\theta)d\Omega$ of finding another galaxy within solid angle $d\Omega$ at an angular separation θ of another galaxy. If we write $P(\theta)d\Omega$ in the form

$$dP(\theta) = \sigma d\Omega[1 + \omega(\theta)], \tag{4.39}$$

where σ is the average *surface*-density of galaxies on the sky, then it is easy to show that

$$\omega(\theta) = \left(\frac{\theta}{\theta_o}\right)^{1-\gamma}, \tag{4.40}$$

where γ is the same index as appears in relation (4.13). If we measure $\omega(\theta)$ we can therefore determine $\xi(r)$.

In Figure 5-8 we show the recently published (November, 2005) *two-point correlation function* $\xi(r)$ from the Sloan Digital Sky Survey extending out to 250 Mpc (using h = 0.72). This plot is remarkable in showing a small enhancement in the *galaxy* correlation on scales around 150 Mpc: this is precisely the scale at which the Cosmic Background Radiation (CBR) asymmetry has a large peak (Figure 1-12, Chapter 1) corresponding to acoustic waves in the early universe 400,000 years after the big bang when the (CBR) photons had decoupled from the matter. What we are seeing is the trace *both* in the galaxy distribution *and* in the CBR of the longest wavelength sound waves in the early universe.

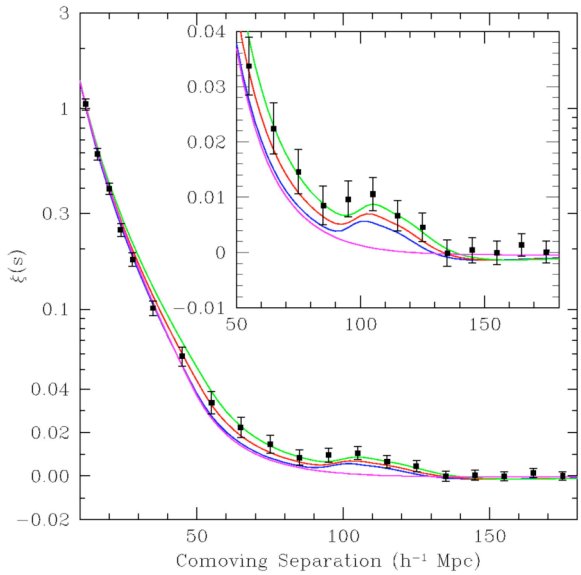

Figure 5-8. the two-point correlation function $\xi(r)$ from the Sloan Digital Sky Survey (ApJ **633**,560,2005)

We can also apply the correlation process to Abell clusters themselves. That is, we can ask for the probability of finding a cluster within a given distance of another. We find that the two-point correlation function $\xi_{\text{intracluster}}(r)$ is of the same form as (4.19):

$$\xi_{\text{intracluster}}(r) = \left(\frac{r}{r_0}\right)^{-\gamma}; \qquad \gamma = 1.8, \quad r_0 = 26\,h^{-1}\ \text{Mpc} \tag{4.41}$$

The power-law exponent is therefore the same as for individual galaxies but the scale-factor is some five times as great. This result emphasises that clustering, at least as described by the two-point correlation function, is a universal phenomenon.

Bibliography for Chapter 5

[1] Longair, M S, *Galaxy formation*, Springer 1998 ISBN 3 54063785 0
[2] Oemler, G., *ApJ* **194** (1974).
[3] Fairall, A P, *Large Scale Structures in the Universe*, Praxis 1998 ISBN: 0 47196253 8